Journal Pre-proof

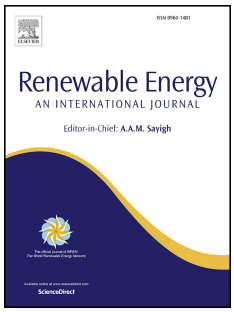

Experimental characterization of a photovoltaic solar-driven cooling system based on an evaporative chimney

J. Ruiz, P. Martínez, H. Sadafi, F.J. Aguilar, P.G. Vicente, M. Lucas

PII: S0960-1481(20)31028-4

DOI: https://doi.org/10.1016/j.renene.2020.06.111

Reference: RENE 13788

To appear in: *Renewable Energy*

Received Date: 21 November 2019

Revised Date: 25 May 2020

Accepted Date: 22 June 2020

Please cite this article as: Ruiz J, Martínez P, Sadafi H, Aguilar FJ, Vicente PG, Lucas M, Experimental characterization of a photovoltaic solar-driven cooling system based on an evaporative chimney, *Renewable Energy* (2020), doi: https://doi.org/10.1016/j.renene.2020.06.111.

J. Ruiz: Conceptualization, Methodology, Formal analysis, Investigation, Data Curation, Writing - Original Draft, Writing - Review & Editing, Supervision, Funding acquisition

P. Martínez: Methodology, Formal analysis, Data Curation, Writing - Review & Editing, Funding acquisition.

H. Sadafi: Methodology, Formal analysis, Data Curation, Writing - Review & Editing, Funding acquisition.

F. Aguilar: Conceptualization, Methodology, Writing - Original Draft, Writing - Review & Editing.

P. Vicente: Conceptualization, Methodology.

M. Lucas: Conceptualization, Methodology, Writing - Original Draft, Writing - Review & Editing.

Experimental characterization of a photovoltaic solar-driven cooling system based on an evaporative chimney

J. Ruiz[a,*], P. Martínez[a], H. Sadafi[b], F.J. Aguilar[a], P.G. Vicente[a], M. Lucas[a]

[a] *Departamento de Ingeniería Mecánica y Energía, Universidad Miguel Hernández, Avda. de la Universidad, s/n, 03202 Elche, Spain*
[b] *TIPs (Transfers, Interfaces and Processes), University Libre of Bruxelles, Av. F.D. Roosvelt 50, Bruxelles, Belgium*

Abstract

Photovoltaic systems combined with electrical compression chillers offer a high potential for energy efficient cooling with a high economic feasibility. They can significantly reduce the energy consumption in the building sector. The main goal of this study is to analyse the performance of a PV solar driven water-water chiller. The novelty of the work relies on the use of a novel system, called photovoltaic evaporative chimney, which aims to increase the efficiency of solar photovoltaic modules by evaporative cooling. The complete solar cooling system consists of four PV panels (1.02 kW_p) and a 3.8 kW refrigeration capacity water-cooled chiller. A systematic study was undertaken and nine sets of experiments were conducted in summer conditions of a Mediterranean climate (Spain). The system's ability to convert the solar energy into refrigeration capacity was observed to be 0.49 on average for the tests performed. The solar contribution (ratio of PV energy consumption to total absorbed energy) was 64.40%. The system produced on average 11.32 cooling kWh per each kWh consumed from the grid. The influence of the ambient conditions on the key performance indicators has been assessed and global correlations for use in more detailed energy analyses have been developed.

Keywords: Solar cooling, Solar chimney, Evaporative cooling, HVAC

1. Introduction

There is important concern in our current society about climatic change and the low level of traditional energy resources, thus it is necessary to develop new, more environmentally friendly technologies that require a minimum level of contribution from fossil fuels. In this sense, main efforts should be focused on buildings because they are responsible for almost 41% of the European Union's final energy consumption and approximately 36% of CO_2 emissions. The latest modification of the Energy Performance of Buildings Directive (EPBD), establishes the commitment of the Union to reduce greenhouse gas emissions further by at least 40% by 2030 as compared with 1990, to increase the proportion of renewable energy consumed, to make energy savings in accordance with Union level ambitions, and to improve Europe's energy security, competitiveness and sustainability. On the path towards the improvement of the energy performance of buildings within the EU, the directive set the target of 100%-share of nearly zero-energy buildings (nZEBs) for new buildings from 2020. Nearly zero-energy buildings have very high-energy performance and the low amount of energy that these buildings require comes mostly from renewable sources. Amongst the different uses for energy in buildings, heating and cooling accounts for 76% of total final energy use in EU households. In southern European countries such as Spain, Italy or Portugal, cooling may constitute up to 50% of the final energy use in the building sector. Accordingly, the heating and cooling demand in the building sector constitutes a major target in the EU's energy efficiency policies due to the potential to lead to significant energy savings and decreasing the CO_2 emissions. Therefore, one action that can be adopted in pursuit of achieving a highly energy-efficient and decarbonised building stock, and ensuring that the long-term renovation strategies deliver the necessary progress towards the transformation of existing buildings into nearly zero-energy buildings, is the development and use of high-efficient energy systems totally or partially driven by renewable (solar) energy. This idea constitutes the main motivation of the present work.

Solar energy can be converted into cooling using two main principles: solar thermal driven cooling and photovoltaic driven cooling. Kim and Ferreira (2008) and Ghafoor and Munir (2015) amongst others, reported a state-of-the-art review of the different technologies available to deliver refrigeration from solar energy. In solar thermal driven cooling, the heat generated with solar thermal collectors can be converted into cooling using thermally driven refrigeration or air-conditioning technologies. Most of these systems use the physical phenomena of sorption in either an open or closed thermodynamic cycle. In photovoltaic driven cooling, the electricity generated by

*Corresponding author. Tel.: +34965222433; fax: +34965222493
Email address: j.ruiz@umh.es (J. Ruiz)

Nomenclature

A	area of the PV panels (m^2)
c_p	specific heat (J kg^{-1} K^{-1})
EER	heat pump energy efficiency ratio, $EER = \dot{Q}_{evap}/\dot{W}_{comp}$
EER_G	system energy efficiency ratio, $EER_G = \dot{Q}_{evap}/\dot{W}_G$
EER_{grid}	grid energy efficiency ratio, $EER_{grid} = \dot{Q}_{evap}/\dot{W}_G^{grid}$
EER_S	solar energy efficiency ratio, $EER_S = \eta_{PV}\, EER_G\, PF$
G	irradiance (W m^{-2})
h	enthalpy (J kg^{-1})
h_e	external heat transfer coefficient (W m^{-2} K^{-1})
h_i	internal heat transfer coefficient (W m^{-2} K^{-1})
h_{s_w}	enthalpy of saturated air at water temperature (J kg^{-1})
h_v	enthalpy of vaporization (J kg^{-1})
k	thermal conductivity (W m^{-1} K^{-1})
Le	Lewis number (-)
$\dot{m}$	mass flow rate (kg s^{-1})
Me	Merkel number (-)
PF	production factor, $PF = \dot{W}_G^{PV}/\dot{W}_{PV}$
$\dot{Q}$	heat rate (W)
Q	volumentric flow rate (m^3 s^{-1})
q_c	heat rate transmitted to the cells (W)
SC	solar contribution, $SC = \dot{W}_G^{PV}/\dot{W}_G$
T	temperature (°C)
T_m	PV module temperature (°C)
T_{ref}	reference temperature (°C)
T_{wb}	wet bulb temperature (°C)
t	time (s)
v_w	wind velocity (m s^{-1})
$\dot{W}$	power (W)
w	humidity ratio (kg_v kg_a^{-1})
$\dot{W}_G$	system power consumption (W)
$\dot{W}_G^{grid}$	grid power consumed by the system (W)
$\dot{W}_G^{loss}$	PV power lost (W)
$\dot{W}_G^{PV}$	PV power consumed by the system (W)
$\dot{W}_{PV}$	power generated by the panels (W)
w_{s_w}	humidity ratio of saturated air at water temperature (kg_v kg_a^{-1})
X	dimensionless q_c dissipated in the panel's front face (-)
x	thickness (m)

Greek symbols

β	efficiency correction coefficient for temperature (°C^{-1})
η_{PV}	electrical efficiency of the PV panels, $\eta_{PV} = \dot{W}_{PV}/GA$
$\eta_{PV_{ref}}$	module's electrical efficiency coefficient (-)
λ	solar radiation coefficient (-)
ϕ	relative humidity (-)
Θ	dummy variable used in the power/energy analysis (-)

Subscripts

1	inlet
2	outlet
a	air
amb	ambient
C	rear side of the PV panel
comp	compressor
cond	condenser
evap	evaporator
g	glass
heaters	heaters
int	outlet section of evaporative area
pump	pump
s	silicon
t	tedlar
w	water

Abbreviations

PCM	Phase Changing Materials
PV	Photovoltaic

photovoltaic cells can be converted into cooling using well-known refrigeration technologies that are mainly based on vapour compression cycles.

Several studies can be found in the literature comparing the performance of different solar cooling technologies. Kim and Ferreira (2008) conducted a comparison between different solar cooling solutions both from the point of view of energy efficiency and economic feasibility. They estimated higher savings for the photovoltaic driven cooling scheme for panel costs ranging 4-7 € W^{-1}. The most detailed study found in the bibliography is the work conducted by Fong et al. (2010). The authors compared five different solar cooling systems: solar electric compression refrigeration, solar mechanical compression refrigeration, solar absorption refrigeration, solar adsorption refrigeration and solar solid desiccant cooling. They found that solar electric compression refrigeration and solar absorption refrigeration had the highest energy saving potential in a subtropical city (Hong Kong) and highlighted the higher efficiency and the lower technical complexity of the PV solar system. Otanicar et al. (2012) performed a technical and economic comparison of several solar cooling approaches, including both thermally and electrically driven. They concluded that, from an environmental standpoint, solar electric cooling had a lower projected emission value of CO_2 per kWh of cooling than any of the thermal technologies. The authors accurately predicted the decrease of PV manufacturing and installation costs. Hartmann et al. (2011) presented a comparison of solar thermal and solar electric cooling for a typical small office building exposed to two different European climates (Freiburg and Madrid). With the assumptions made in their work, the authors concluded that the grid coupled PV system led to lower costs and higher primary energy savings than the solar thermal system at both locations. Lazzarin (2014) performed a thermodynamic and economical analysis of PV and thermal solar cooling systems. They estimated that with the decrease in the costs and the increase in the efficiency, the

PV driven heat pump systems constitute a competitive alternative to thermal collectors and thermal compression systems. More recently, Lazzarin and Noro (2018) carried out an energy/economic comparison for various solar cooling systems, including PV driven and solar thermal driven. They concluded that, in terms of costs of investment, the nowadays situation favours decidedly PV driven technologies. They also stated that a similar cooling production can be supplied by PV driven systems at a cost about a half than for the best thermally driven. Similar conclusions were reached by Eicker et al. (2015). The authors conducted a systematic simulation study to evaluate the overall performance of PV compression cooling systems in office buildings for different climatic conditions worldwide. They concluded that the primary energy savings for solar electric cooling and heating were comparable to solar thermal systems and, even more advantageous, if grid export is possible and paid for.

So far, the literature review has highlighted the difficulty for solar thermal cooling to emerge as a competitive solution due to technical and economic reasons. Therefore, according to the literature survey carried out and to the International Energy Agency-New generation solar cooling & heating systems task, photovoltaic (PV) driven compression systems are the most promising and close to market solar solution today in the case of small to medium units, Mugnier et al. (2015). Solar-driven heat pumps can reduce significantly the primary energy consumption in buildings by improving the efficiency of conventional HVAC systems, Al-Alili et al. (2014). Besides, the drop of the costs and the increase of the performance of the panels, make this alternative even more attractive.

One of the major problems issues that is currently limiting the state-of-the-art of solar-driven heat pump systems, is related to the efficient conversion of solar energy due to panel heating. In a traditional polycrystalline silicon PV panel, typically 10-20% of the radiated solar energy is converted into electricity (usually referred to as Power Conversion Efficiency or just electrical efficiency) while the remainder is transformed into heat. This fact causes heating of the solar cells in PV panels resulting in a drop in the conversion rate of about 0.5%/°C, Biwole et al. (2013). In summer periods, where the panel can experience temperatures ranging 40-70°C, the drop of maximum power production can be up to 22%. Consequently, the temperature regulation of photovoltaic panels becomes of high importance to achieve an efficient operation and it can be achieved by the use of active or passive cooling techniques. A detailed compilation of the investigations addressing the reduction of the PV panel temperature can be found in Chandrasekar et al. (2015). Active cooling techniques (use of water and air as coolant agent) often result in significant benefits regarding the PV panel performance, Odeh and Behnia (2009); Teo et al. (2012); Bahaidarah et al. (2013); Kaiser et al. (2014). However, among the major drawbacks pointed out in the literature, the external source of energy consumption to create the fluid flow and the initial investment are found. Phase Changing Materials (PCM) constitute another feasible solution to cool down the panels and improve their efficiency due to the higher energy storage density of such materials. They are classified as passive cooling techniques. The main advantage is the ability to delay the temperature rise of panel without any electricity consumption. Furthermore, the heat stored can be reused which further enhancement of efficiency of the system. The work of Chandel and Agarwal (2017) presents a complete review of studies combining PV and PCM. The limitations stated by the authors are the concern of the cyclic stability of the material and the poor thermal conductivity.

The main goal of this study is to analyse the performance of a PV solar driven water-water chiller in summer conditions of a Mediterranean climate (Spain). The novelty of the work relies on the use of a novel system, called photovoltaic evaporative chimney, which aims to increase the efficiency of solar photovoltaic modules by evaporative cooling. It consists of a solar chimney attached to the rear side of the PV panel that enhances its performance by cooling down the panel due to the buoyancy-driven flow induced in the chimney. Moreover, in the so-called evaporative area, water is sprayed parallel to the downward airflow by a series of nozzles. As the water descends, a small part of it evaporates, cooling the remaining water. This zone works as a small scale cooling tower. The air that has been in contact with water may have reduced its temperature (it will depend on ambient conditions), enhancing the cooling effect in the panel. As the water used for cooling the modules will be available to be used for the condensation of a refrigeration cycle, the system also increases the efficiency of the heat pump (water-cooled system). Hence, the benefits of the photovoltaic evaporative chimney are two-fold.

The system's performance was assessed by Lucas et al. (2017). Authors reported the operation of a system consisting of two PV collectors, one of them used as a reference and the other was modified in its rear side including the evaporative solar chimney. The system was able to dissipate a thermal power of about 1.5 kW with a thermal efficiency exceeding 30% in summer conditions. The PV module temperature differences between the cooled module and the one used as a reference, reached 8°C depending on the wind conditions and ambient air psychrometric properties, yielding to an improvement of the electrical efficiency up to about 8% with respect to nominal efficiencies. In Lucas et al. (2019) the same group of authors investigated the modification of the evaporative photovoltaic chimney performance when a water slide system on the upper face of the photovoltaic panel was added. This modification aimed to overcome some operation issues observed in the first prototype such as the non-uniformity of the module temperatures distribution and the negative effect of high-wind conditions on the operation of the system. The results showed an average cooling of the panel of 15°C and an improvement in the electrical efficiency of

the panel of about 10%. The modified system was still able to dissipate a thermal power of about 1.5 kW with a thermal efficiency exceeding 30% in summer conditions. However, those studies were limited to the investigation of the performance of the panel and the evaporative chimney, not assessing the operation of the system connected to a water-cooled chiller dissipating the heat (thermal load) from a building.

As stated before, the main objective of this work is to experimentally characterize the performance of a PV solar-driven cooling system enhanced with a photovoltaic evaporative chimney. The system consists of four PV panels (1.02 kW_p nominal power) attached to their corresponding evaporative chimneys and a 3.8 kW refrigeration capacity, water-cooled chiller. A systematic study was undertaken and nine sets of experiments were conducted in summer conditions (Mediterranean climate). The system performance was characterized in terms of the photovoltaic panels and the chiller/system performances. Secondary objectives were to evaluate the influence of ambient conditions on the system performance and to develop global correlations for the key performance indicators of the system as a function of the relevant above mentioned parameters. The final use of these correlations is to be included in energy simulation programs to perform more detailed energy analyses.

The paper is structured as follows: Section 2 contains the description of the experimental facility, experimental procedure and the mathematical characterization of the system. In Section 3, the main results of the research and their discussion are presented. Finally, in Section 4 the main conclusions and the future works are described.

2. Material and methods

2.1. Experimental facility

The experimental facility where the experiments were carried out is located on the roof of Torrepinet building, Miguel Hernández University of Elche. As shown in Figure 1, the basis of the solar installation consists of four photovoltaic modules (255 W_p) which rear side have been modified by attaching four evaporative chimneys. The orientation for the PV modules is true south (Azimuth angle 0º) and although the experimental installation is ready to work with 30º, 45º and 60º tilt angles, in the present work is fixed at 45º. The evaporative system chimney have been extensively described in the literature (Lucas et al., 2017, 2019) and its function is twofold: cool the panels down due to the buoyancy-driven flow induced in the convective zone and reject the heat from the condenser of a water-cooled chiller in the evaporative area.

A schematic arrangement of the facility is shown in Figure 2. The PV modules are connected to a grid-tied microinverter with intelligent networking and monitoring systems to ensure maximum efficiency since it has an independent maximum power point control for each module. The energy produced by the panels is self-consumed by the facility (compressor and pump). The remainder energy required to power the system is consumed from the grid. In the case that the production exceeds the demand, the energy is dissipated by means of an electrical resistance of 1500 W to avoid injecting the electrical energy produced by the PV modules into the grid.

The water-cooled inverter heat pump was designed on purpose for this application. It has a nominal cooling capacity of 3.8 kW. In this conditions, the rotary compressor absorbs 0.9 kW.

Two hydraulic circuits are connected to the heat pump. The hot loop is connected to the condenser and is composed of a network of PVC pipes. The flow is driven from the tank to the nozzles arranged linearly in the input section of the solar chimney by a centrifugal pump. The 28 flat spray nozzles (spray angle 110º) atomize the water evenly. The sprayed water mass flowrate can be changed manually by means of a balancing valve. In the cold loop, connected to the evaporator, the water is circulated by a hydraulic pump. It is made of a series of multilayer pipes thermally insulated. Three electrical heaters (2 x 1.4 kW and 1 kW) were used to simulate a building thermal load.

To experimentally analyze the thermal and electrical performance of the photovoltaic evaporative chimney a series of variables were monitored and recorded. The first group of sensors are responsible for measuring environmental conditions: ambient air temperature, air relative humidity, wind speed and wind direction all of them are measured with a meteorological station placed on the laboratory roof just beside the experimental facility. A pyranometer is used to measure radiation. This sensor is classified as First Class by the standard ISO 9060 (ISO, 2018), and is installed in the same plane of the PV modules to measure radiation. Twelve K-type thermocouples were installed on the rear side of the PV modules (3 on each module) distributed at three different heights in the centreline of the modules to measure their surface temperature. The voltage of each panel is directly measured while the current is determined via the voltage drop produced in a shunt resistance. To evaluate the thermal performance of the system, the following variables were measured: air temperature and relative humidity at the transition point between the evaporating section and the convective section and at the output section, air velocity inside the solar chimney, inlet and outlet water temperatures in each loop, water mass flows and supply water. All the data recorded during the experiments was monitored by an Agilent 34972A data-acquisition system. The sensors used during the experiment are shown in Figure 3.

2.2. Experimental procedure

Nine sets of experiments were conducted during the months of July and August of 2018. The duration of the tests was 10 h on average (from 9 am to 6-7 pm). Table 1 shows the averaged values of the most relevant ambient conditions during the tests. In all the tests, the water

flowrates in the condensing and evaporative loops, respectively, were maintained at the nominal values for the operation of the solar chimney (∼2000 l h^{-1}) and the chiller (654 l h^{-1}).

In order to achieve steady operating conditions for all the variables, including temperatures, a startup period of 30 minutes was considered. From that moment, the prototype was working from early morning until late afternoon. UNE-EN 12975-2 "Thermal solar systems and components- Solar collectors - Part 2: Test methods" and Standard UNE 13741 "Thermal performance acceptance testing of mechanical draught series wet cooling towers" were selected as reference to define stationary conditions. For a test to be valid, variations in the test conditions shall be within the following limits during a 10 minutes period. The variations of the circulating water flow rate shall not be greater than 5%. The maximum deviation of the wet-bulb temperature may not exceed its average value during the test period (±1.5°C). The same is valid for the dry-bulb temperature with a deviation of (±4.5°C) and water temperatures (±1.5°C). The wind velocity shall not exceed 7 m s^{-1} for 1 minute and its average value during the test period shall not exceed 3.5 m s^{-1}. Global solar irradiance was over 700 W m^{-2} and deviation from the mean less than (±50 W m^{-2}).

2.3. Mathematical characterization

A mathematical characterization of the novel solar cooling system is provided in this section. The solar collectors are characterized via their electrical efficiency (i.e. ratio of electric power generated to total available energy), defined in Eq. (1):

$$\eta_{\mathrm{PV}} = \frac{\dot{W}_{\mathrm{PV}}}{GA} \tag{1}$$

The performance of the photovoltaic evaporative chimney can be studied by dividing the system into two different areas: the evaporative area and the convective area. The link between these two different zones is the temperature of the air leaving the evaporative area (which matches the air temperature entering the convective area). The convective area is characterized by the 1D energy balance in the solar plate. The solar collectors convert the heat rate emitted by the sun into electric power. A portion of this heat rate is absorbed, another portion is reflected and the remainder is transmitted to the collector cells (q_c). A part of q_c is converted into electricity and the remainder is transformed into heat, which is dissipated in the front and rear sides of the panel by means of convection. The heat not evacuated causes heating of the solar cells in PV panels resulting in a drop in the conversion rate. The energy balance in the solar plate is shown in (2), where the subscripts g, s, t, and C refer to the temperatures of the glass, silicon, tedlar, and rear side of the panels, respectively.

$$\begin{aligned}
X q_c &= h_e A \left(T_g - T_{\mathrm{amb}}\right) \\
X q_c &= \frac{A k_g}{x_g} \left(T_s - T_g\right) \\
(1-X)\, q_c &= \frac{A k_s}{x_s} \left(T_s - T_t\right) \\
(1-X)\, q_c &= \frac{A k_t}{x_t} \left(T_t - T_C\right) \\
(1-X)\, q_c &= h_i A \left(T_C - T_{\mathrm{int}}\right)
\end{aligned} \tag{2}$$

In the evaporative area of the evaporative solar chimney, heat and mass between water and air are transferred. Water flows downwards from the nozzles to the tower basin (where is finally collected) in parallel to the air stream (parallel flow arrangement). The major equations for the heat and mass transfer in the evaporative area have been adapted from Poppe and Rögener (1991) and Kloppers and Kröger (2005) for counterflow arrangement.

$$\begin{aligned}
&\tfrac{dw}{dT_w} = c_{p_w} \tfrac{\dot{m}_w}{\dot{m}_a} \left(w_{s_w} - w\right) \\
&\quad \frac{1}{h_{s_w} - h + (\mathrm{Le}-1)\left[h_{s_w} - h - \left(w_{s_w} - w\right) h_v\right] - \left(w_{s_w} - w\right) c_{p_w} T_w} \\
&\tfrac{dh}{dT_w} = \tfrac{\dot{m}_w c_{p_w}}{\dot{m}_a} \\
&\quad \left(1 + \frac{\left(w_{s_w} - w\right) c_{p_w} T_w}{h_{s_w} - h + (\mathrm{Le}-1)\left[h_{s_w} - h - \left(w_{s_w} - w\right) h_v\right] - \left(w_{s_w} - w\right) c_{p_w} T_w}\right) \\
&\tfrac{d\,\mathrm{Me}}{dT_w} = c_{p_w} \frac{1}{h_{s_w} - h + (\mathrm{Le}-1)\left[h_{s_w} - h - \left(w_{s_w} - w\right) h_v\right] - \left(w_{s_w} - w\right) c_{p_w} T_w}
\end{aligned} \tag{3}$$

Finally, the chiller is characterized by the power balance and the energy efficiency ratio (EER), defined as the ratio of the absorbed heat rate in the evaporator to the power absorbed in the compressor,

$$\begin{aligned}
\dot{Q}_{\mathrm{cond}} &= \dot{Q}_{\mathrm{evap}} + \dot{W}_{\mathrm{comp}} \\
\mathrm{EER} &= \frac{\dot{Q}_{\mathrm{evap}}}{\dot{W}_{\mathrm{comp}}} = \frac{\dot{Q}_{\mathrm{cond}} - \dot{W}_{\mathrm{comp}}}{\dot{W}_{\mathrm{comp}}}
\end{aligned} \tag{4}$$

where the heat rates absorbed and rejected in the evaporator and the condenser, respectively, are displayed in Eq. (5):

$$\dot{Q} = \dot{m} c_p \Delta T \tag{5}$$

Here, the mass flowrate, specific heat, and temperature difference refer to the cold and hot loops, respectively.

Once the mathematical model of the cooling system has been stated, the following key performance parameters are defined to characterize the system's performance. They can be calculated in power or energy basis. For the energy analysis, the conversion from power data in kW to energy data in kWh can be done by summing every instant magnitude multiplied by the time step. Eq. (6) shows the general conversion procedure from power to energy, where

Test run	Date	Thermal load (kW)	Temperature (°C)	Relative humidity (%)	Wet-bulb temperature (°C)	Irradiance (W m^{-2})	Wind velocity (m s^{-1})
1	17/07/2018	2.71	29.99	40.81	20.22	611.12	3.47
2	23/07/2018	2.29	32.20	69.61	27.44	611.93	2.47
3	25/07/2018	2.23	28.43	68.57	23.85	629.51	2.86
4	27/07/2018	2.63	29.79	60.59	23.73	688.46	2.41
5	30/07/2018	2.28	30.15	66.70	25.09	612.67	2.75
6	31/07/2018	2.32	31.25	61.25	25.12	703.23	2.34
7	03/08/2018	2.19	32.64	46.32	23.44	589.54	2.50
8	04/08/2018	2.28	32.92	42.32	22.82	619.25	2.23
9	07/08/2018	2.24	31.20	56.67	24.25	627.98	2.50

Table 1: Daily averaged values in the experimental test runs conducted.

Θ denotes any magnitude involved in the analysis and Δt refers to the time step used in the measurements.

$$\Theta = \sum \dot{\Theta} \Delta t \tag{6}$$

As previously described, the power generated by the panels can be used to drive the system (compressor and hot loop pump, $\dot{W}_G = \dot{W}_{\text{comp}} + \dot{W}_{\text{pump}}$) totally or partially. The quantities $\dot{W}_G^{\text{PV}}$, $\dot{W}_G^{\text{grid}}$, and $\dot{W}_G^{\text{loss}}$ refer to the PV power consumed by the system, amount of power consumed from the grid, and generated PV power lost, respectively. Two possible scenarios could be expected in the operation of the system depending on the difference between the panels generation and the system's consumption ($\dot{W}_{\text{PV}} - \dot{W}_G$): excess of renewable energy production and system power demand exceeding generation. When $\dot{W}_{\text{PV}} > \dot{W}_G$ (i.e. excess of renewable energy production), then $\dot{W}_G^{\text{PV}} = \dot{W}_G$, $\dot{W}_G^{\text{grid}} = 0$, and $\dot{W}_G^{\text{loss}} > 0$. In the other possible scenario (the system power demand exceeds the generation, $\dot{W}_{\text{PV}} < \dot{W}_G$), then $\dot{W}_G^{\text{PV}} = \dot{W}_{\text{PV}}$, $\dot{W}_G^{\text{grid}} > 0$, and $\dot{W}_G^{\text{loss}} = 0$. Figure 2 includes the power quantities related to each component.

The contribution of solar energy or just the solar contribution, SC, is defined as the ratio of the renewable energy consumed by the compressor coming from the panels to the total energy,

$$\text{SC} = \frac{\dot{W}_G^{\text{PV}}}{\dot{W}_G} \tag{7}$$

The production factor, PF, relates the panels' power generation and the system's power consumption. It is a measure of the use of renewable energy driving the compressor and the pump,

$$\text{PF} = \frac{\dot{W}_G^{\text{PV}}}{\dot{W}_{\text{PV}}} \tag{8}$$

It accounts for those intervals of operation when the PV generation is not used in the facility.

The global energy efficiency ratio (EER_G), Eq. (9), takes into account the system's ability to convert the global energy (electricity) consumption to cooling,

$$\text{EER}_G = \frac{\dot{Q}_{\text{evap}}}{\dot{W}_G} = \frac{\dot{Q}_{\text{evap}}}{\dot{W}_{\text{comp}} + \dot{W}_{\text{pump}}} \tag{9}$$

The pump power consumption is included in Eq. (9) since the circulating pump placed in the condenser loop is part of the solar cooling system.

The grid energy efficiency ratio (EER_{grid}), Eq. (10), indicates the grid electricity needed for producing the energy demand. This parameter calculated on an energy basis can be considered as a mean EER, but in working conditions.

$$\text{EER}_{\text{grid}} = \frac{\dot{Q}_{\text{evap}}}{\dot{W}_G^{\text{grid}}} \tag{10}$$

Finally, the solar energy efficiency ratio (EER_S), Eq. (11), is a parameter which relates the refrigeration capacity obtained using renewable energy to the total incoming irradiated heat rate. It is a measure of the system's ability to convert the solar energy into refrigeration capacity. Hence, it can be very useful when comparing different solar cooling systems. For the studied system, the EER_S can be related to the product of the system and panels efficiency to the production factor.

$$\text{EER}_S = \frac{\dot{Q}_{\text{evap}_{\text{PV}}}}{GA} = \eta_{\text{PV}}\, \text{EER}_G\, \text{PF} \tag{11}$$

Most of the key performance indicators mentioned above have been adapted from the report of the International Energy Agency-New generation solar cooling & heating systems task 53, Aguilar et al. (2018). Authors focus on the testing and the monitoring methodology to measure the performances of field tests of compression heat pumps driven by photovoltaic solar energy.

3. Results and discussion

The results obtained from the nine experiments presented in this paper, are described in this section. For comprehensively describing the test runs, this section has been divided into three parts: test description, tests results, and trends and discussion. In each one of them, the ambient conditions results, panels and heat pump performance, efficiency parameters results, and global energetic results are presented separately.

3.1. Test description

This section presents the results obtained taking as an example the experiment carried out on July 27, 2018 (test run number 4, Table 1).

3.1.1. Ambient conditions

Figure 4 depicts the variation of the ambient conditions during the test. The green shaded area represents the stationary intervals. As it can be observed in Figure 4(a), it was a completely clear day in which the irradiance exceeded 900 W m^{-2} at midday. This figure also includes the measurements of wind velocity, with an average value throughout the whole test of 2.41 m s^{-1}. It is noted that the wind velocity at the start of the day was low and, as the day progressed, its value increased with wind gusts exceeding 3 m s^{-1}. Figure 4(b) shows ambient air temperature and relative humidity, which ranged between 29.04-31.31°C and 50.10-66.32%, respectively.

3.1.2. Photovoltaic panels

The performance of the PV panels is depicted in Figure 5. Figure 5(a) shows the variation of the temperature distributions on the back surface of the photovoltaic modules (average of the 4 panels at each section: upper, middle and lower) and the global irradiance. The combined effect of the solar irradiance and the wind speed affects the module temperature. The temperature changes respond to the irradiance variation throughout the day, deviating occasionally due to gusts of wind dissipating the heat in the front side of the panels due forced convection. The temperature stratification observed is because of the heating of the air circulating inside the chimney. No relevant temperature difference is observed between upper and middle sections. Temperature differences up to 8.40°C are observed between upper and lower sections.

Figure 5(b) presents the evolution of the generated power by the panels as well as their efficiency during the test. The four PV panels supply 758.37 W at midday. The maximum generation of each panel ranges from 185.96 to 195.31 W. The instant performance of the four panels slightly changes throughout the day ranging from 12.71% to 13.64%. This maximum instant value was registered at the beginning of the test. The factors affecting the generation the most are the temperature of the panels and the global irradiance. The fact that the registered temperatures are above the standard test conditions temperature ($T_{\mathrm{ref}} = 25$°C) and the irradiance is different than 1000 W m^{-2} results in a decrease in the power generation and the efficiency with respect to manufacturer data (255 W and 15.67%).

3.1.3. Heat pump performance and efficiency parameters

The next group of results shown in Figure 6 concerns the heat pump performance and efficiency parameters. Figure 6(a) shows the operation of the evaporator and the condenser (temperatures difference and water volumetric flowrates), respectively. Figure 6(b) presents the power balance in the system and the efficiency parameters. As it can be observed, the evaporator dissipates the heat rate gained in the cold loop, which is about 3.4 kW (electrical heaters and circulating pump). The power absorbed by the compressor is about 0.6 kW and the heat rate rejected in the condenser is 4 kW. The right-side of Figure 6(b) depicts the efficiency parameters of the system. The instant values, found mainly constant during the test, are EER = 5.15, $\mathrm{EER}_G = 4.28$ and $\mathrm{EER}_S = 0.54$. These results exceed the typical efficiencies achieved by other solar cooling systems (i.e. PV panels and air-cooled heat pump or solar panels and absorption chillers), which according to the literature are about 0.20-0.43, Martínez et al. (2012); Aguilar et al. (2019).

The average experimental uncertainty for the key performance indicators during the stationary intervals was $\eta_{\mathrm{PV}} = 0.1279 \pm 0.0021$ (1.6%), $\mathrm{EER} = 5.15 \pm 0.14$ (2.7%), $\mathrm{EER}_G = 4.28 \pm 0.12$ (2.8%) and $\mathrm{EER}_S = 0.54 \pm 0.02$ (3.2%), respectively. It was calculated according to ISO Guide (ISO, 1993) with a level of confidence of 95% using the sensor specifications.

3.1.4. Global energetic results

The electrical and thermal energy flows produced in the facility are calculated in a daily basis from the data measured every 10 seconds (3324 data in almost 10 hours). They are shown in an hourly basis in Table 2.

Interval	Q_{cond}	Q_{evap}	W_{comp}	W_G	W_{PV}	GA	W_G^{PV}	W_G^{loss}	W_G^{grid}
10-11 h	1.91	1.63	0.32	0.42	0.35	2.57	0.29	0.06	0.13
11-12 h	3.96	3.35	0.64	0.77	0.59	4.44	0.59	0.00	0.18
12-13 h	3.99	3.35	0.65	0.78	0.69	5.28	0.69	0.00	0.10
13-14 h	4.03	3.39	0.67	0.80	0.74	5.79	0.74	0.00	0.05
14-15 h	4.10	3.42	0.68	0.81	0.75	5.84	0.75	0.00	0.06
15-16 h	4.10	3.44	0.67	0.80	0.71	5.55	0.71	0.00	0.09
16-17 h	4.06	3.41	0.66	0.79	0.62	4.86	0.62	0.00	0.17
17-18 h	4.04	3.40	0.66	0.79	0.48	3.80	0.48	0.00	0.31
18-19 h	4.06	3.41	0.65	0.78	0.29	2.46	0.29	0.00	0.50
19-20 h	1.97	1.67	0.32	0.38	0.06	0.70	0.06	0.00	0.31
10-20 h	36.20	30.48	5.92	7.12	5.28	41.29	5.22	0.06	1.90

Table 2: Hourly and daily data obtained in the energy analysis (kWh) for test run number 4.

In a typical summer day in a Mediterranean climate, the four PV panels of this facility produce 5.28 kWh with an efficiency of 12.79%. This value can be interpreted as the area under the curve of the PV generation during the test, Figure 7.

The peak efficiencies are observed for the 10-13 h interval (13.02-13.58%). The daily value is slightly lower due to the poor efficiencies achieved mainly due to increase in the reflected radiation because of the solar incidence angle.

The overall system energy consumption is 7.12 kWh. The compressor accounts for the 83.13% of this consumption (5.92 kWh) while the remainder is used to power the hot loop pump. The solar contribution is, therefore, 73.36%. The maximum value (93.33%) is observed in the interval 13-14 h when the difference between PV generation and the total consumption of the system is minimum. The lowest solar contribution (17.04%) is found between 19 h and 20 h.

The system absorbs all the energy generated by the panels except for some periods in the 10-11 h interval. During this interval, 0.06 kWh are lost (dissipated in the

electrical resistance), lowering the production factor to 0.82. The production factor for the rest of the intervals is 1, while the daily production factor is 98.83%. A total amount of 1.90 kWh are provided by the grid, as the panels cannot drive totally the system.

The operation of the whole system is characterized by the key performance indicators described in Section 2.3. In this sense, the system's ability to convert electricity into refrigeration is measured by the heat pump and system EER. The calculated values are EER = 5.15 and $\text{EER}_G = 4.28$, which roughly match the instant values. The latter result means that the system is able to produce 4.28 kWh for each electric kWh absorbed. When the panels generation is taken into account in the analysis, a $\text{EER}_{\text{grid}} = 16.07$ is obtained. This value represents the amount of cooling produced (16.07 kWh) per each 1 kWh of electricity coming from the grid. Finally, the calculated solar EER, $\text{EER}_S = 0.54$ indicates the conversion of 1 kWh of incoming irradiated energy to 0.54 kWh refrigeration capacity.

3.2. Tests results

In this section, the results of the nine experimental tests carried out at the pilot plant are presented, taking as a reference Section 3.1. Again, for the clarity and coherency of the paper, the most relevant parameters in the experimental investigation are presented in Figure 8: the photovoltaic panels efficiencies, and heat pump and system performances. The presented results correspond to the values calculated on a daily basis (energy). They are shown in Table 3.

Concerning the variation of the efficiency of the panels in the tests, it varies in the range 12.41-12.79%. As the irradiance level is similar for all the tests, the efficiency is mainly affected by the modules temperature. The lowest efficiencies are observed for test runs 2, 3, and 9 according to this fact.

The performance of the heat pump and the system is depicted via the EER, EER_G, and EER_S. It can be observed that the heat pump EER falls within the range of 4.14-5.15. The use of water as condensing media explains this high performance indicator. The system's performance is calculated by taking into account the consumption of the condensing pump. Its value is found between 3.52-4.28. Both of these indicators are strongly affected by the condensing/wet-bulb temperature, which justifies the lower performances for test runs 2, 6, and 9.

The calculated values for the solar energy efficiency ratio range from 0.44-0.54.

The production factor and the solar contribution experience slightly changes between tests. Generally speaking, the system uses all the renewable energy generated by the panels to drive the compressor and the pump (PF $\approx$ 1). This amount of energy supplies from a 57.68% to a 73.33% of the total energy consumption (solar contribution). The most relevant indicator in this analysis is the EER_{grid}, which ranges from 8.31-16.07.

3.3. Trends and discussion

The influence of the environmental conditions on the PV panels and the system performance is evaluated in this section.

As discussed previously, the factors affecting the electrical efficiency the most are the temperature of the PV modules and the irradiance. As suggested by Skoplaki and Palyvos (2009), the electrical performance of the panels as a function the temperature and the irradiance can be correlated as shown in Eq. (12). The efficiency correction coefficient for temperature (β), is normally given by the PV manufacturer ($\beta = 0.0044$ 1/°C for the panels studied in this work and $T_{\text{ref}} = 25$°C) and remains constant regardless of the module temperature and the irradiance. The other coefficients in Eq. (12) have been determined by fitting the equation to the experimental data. The calculated values for them are $\eta_{\text{PV}_{\text{ref}}} = 0.1447$ and $\lambda = 0.02748$. The difference between the calculated maximum efficiency value and the provided by the manufacturer (0.1567) can be attributed to several reasons such as the aging of the panels.

$$\eta_{\text{PV}} = \eta_{\text{PV}_{\text{ref}}} \left[1 - \beta\left(T_C - 25\right) + \lambda \log_{10}\left(\frac{G}{1000}\right)\right] \quad (12)$$

Figure 9 depicts the effect on the ambient conditions on the panels' efficiency. Since the irradiance has shown a lower impact on the efficiency than the module temperature (at least for the range of irradiances studied in this work), the relationship between the latter and the electrical efficiency is plotted. The correlation is presented along the experimental data, showing an excellent agreement. The average irradiance value for the data presented ($\bar{G} = 888.78$ W m^{-2}) was used in the plot.

Figure 10 shows the influence of operating conditions on the efficiency of the chiller, represented by EER_G. The chiller operation depends mainly on condensation and evaporation temperatures, T_{cond} and T_{evap}. The condensing and evaporating temperatures were not registered during the experimental tests. Hence, the condenser inlet water temperature ($T_{w_{1_{\text{cond}}}}$) and the evaporator outlet water temperature ($T_{w_{2_{\text{evap}}}}$) were used instead. In this study, the evaporator outlet water temperature was almost constant during the tests and roughly equal to 7°C, as in typical air conditioning applications. Therefore, the performance of the system EER_G is depicted against $T_{w_{1_{\text{cond}}}}$. A linear relationship is observed between them. The slope and the y-intercept for the linear regression are -0.09153 1/°C and 6.772, respectively (Eq.(13)). The goodness of the fit is assessed by plotting it alongside the experimental data in Figure 10.

$$\text{EER}_G = 6.772 - 0.09153 T_{w_{1_{\text{cond}}}} \quad (13)$$

As stated in the introduction section, secondary objectives of this work were to evaluate the influence of ambient conditions on the system performance and to develop

Test run	Q_{cond}	Q_{evap}	W_{comp}	W_G	W_{PV}	GA	W_G^{PV}	W_G^{loss}	W_G^{grid}	η_{PV}	SC	PF	EER	EER_G	EER_S	EER_{grid}
1	41.13	34.09	6.82	8.15	5.19	40.69	5.17	0.026	2.98	0.1276	0.634	0.995	5.00	4.18	0.53	11.43
2	39.10	31.90	7.70	9.07	5.24	41.74	5.23	0.014	3.84	0.1256	0.577	0.997	4.14	3.52	0.44	8.31
3	37.51	31.02	6.502	7.80	5.05	40.69	4.94	0.113	2.86	0.1241	0.633	0.978	4.77	3.98	0.48	10.84
4	36.20	30.48	5.925	7.12	5.28	41.29	5.22	0.061	1.90	0.1279	0.734	0.988	5.15	4.28	0.54	16.08
5	39.74	32.61	7.02	8.35	5.08	40.69	5.06	0.016	3.29	0.1248	0.606	0.997	4.65	3.91	0.49	9.92
6	34.43	28.12	6.07	7.23	5.18	40.86	5.18	0.000	2.05	0.1269	0.717	1.000	4.63	3.89	0.49	13.71
7	41.59	34.04	7.15	8.61	5.44	42.89	5.43	0.012	3.18	0.1269	0.631	0.998	4.76	3.96	0.50	10.71
8	35.95	29.46	6.16	7.43	5.05	39.56	5.04	0.017	2.40	0.1277	0.677	0.997	4.78	3.96	0.50	12.28
9	37.72	30.09	7.19	8.46	4.97	39.99	4.97	0.000	3.49	0.1243	0.587	1.000	4.19	3.55	0.44	8.61

Table 3: Daily data obtained in the energy analysis (kWh) in all the tests performed.

global correlations for the key performance indicators of the system as a function of the relevant ambient parameters. The final use of these correlations is to be included in energy simulation programs to perform global energy analyses. So far, the correlations presented in Eq. (12) and Eq. (13) depend on operating parameters rather than ambient parameters. In the case of the convective area of the evaporative chimney performance, ambient conditions determine the module temperature, T_C, through the set of equations displayed in (2). Therefore, by solving this set of algebraic equations, Eq. (12) is directly linked to the ambient conditions. Refer to Ruiz et al. (2019) for the complete calculation procedure, including the convections coefficients determination and the major assumptions made. The link between operating ($T_{w_{1_{\text{cond}}}}$) and ambient conditions for the evaporative area of the evaporative chimney is more complex. They are related through the Poppe model (Poppe and Rögener, 1991), set of differential equations shown in Eq. (3). The dimensionless number referred to as Me defined in Eq. (3), is the Merkel number according to the Poppe theory. This number is accepted as the coefficient of performance of an evaporative device since it measures the degree of difficulty of the mass transfer processes taken place in the evaporative zone exchange area. The set of coupled ordinary differential and algebraic equations can be solved simultaneously to provide the air humidity, the air enthalpy, the water temperature, the water mass flow rate and the Me profiles in the evaporative area of the chimney. The above described governing equations can be solved by the fourth order Runge-Kutta method. The Merkel number corresponding to different operating conditions can be correlated in terms of the water-to-air mass flow ratio. In the case of the evaporative area of the prototype, the experimental relationship determined by Lucas et al. (2017) can be used to close the system of equations and link Eq. (13) with the ambient conditions.

4. Conclusions

In this paper, a systematic study regarding the experimental characterization of a PV solar-driven cooling system enhanced with a photovoltaic evaporative chimney is presented. A power and an energy analysis have been conducted. The key performance indicators used in both analyses have been adapted from the literature. The results obtained during the experimental investigation can be summarized as follows:

- The solar cooling system achieves, on average for all the tests performed, an electrical efficiency of 12.62% and global EER of 3.91. Both magnitudes are higher than traditional air-cooled, PV-driven heat pumps.
- The system's ability to convert solar energy into cooling capacity is 0.49 on average, exceeding the typical efficiencies achieved by other solar cooling systems, either PV-driven or thermal-driven.
- The test averaged solar contribution, or ratio of PV to total energy consumption, was found to be 64.40%. This magnitude exceeds 90% during the hottest periods of the day, reducing the primary energy consumption and improving the carbon footprint.
- The average grid energy efficiency ratio of the system, is 11.32. That magnitude relates the refrigeration capacity produced when using 1 kWh coming from the grid.
- The electrical efficiency of the panels is mainly affected by the module temperature and the global irradiance, while the heat pump/system performance depends on the condensing and evaporating temperatures.
- Correlations for the key performance indicators as a function of the relevant ambient parameters have been obtained based on the mathematical model developed. They show a good agreement with the experimental results and can be used in global energy analyses.

Future research should consider the potential effects of the tilt angle of the panels on the system performance more carefully. Also, in future work, investigating the effect of the wind direction on the results might prove important.

5. Acknowledgements

The authors acknowledge the financial support received from the Government of Valencia, through the project

GV/2019/008 (Subvenciones para la realización de proyectos de I+D+i desarrollados por grupos de investigación emergentes). The authors wish to acknowledge the collaboration in the experimental work of the following Mechanical Engineering students: Aarón Boix Agulló, José Coves Díez, Patricia Ortega Antón, and, especially, to Eugenio Sánchez Gonzálvez for his amazing work as a lab technician.

References

D. Kim, C. I. Ferreira, Solar refrigeration options – a state-of-the-art review, International Journal of Refrigeration 31 (1) (2008) 3 – 15, ISSN 0140-7007, URL http://www.sciencedirect.com/science/article/pii/S0140700707001478.

A. Ghafoor, A. Munir, Worldwide overview of solar thermal cooling technologies, Renewable and Sustainable Energy Reviews 43 (2015) 763 – 774, ISSN 1364-0321, URL http://www.sciencedirect.com/science/article/pii/S1364032114010120.

K. Fong, T. Chow, C. Lee, Z. Lin, L. Chan, Comparative study of different solar cooling systems for buildings in subtropical city, Solar Energy 84 (2) (2010) 227 – 244, ISSN 0038-092X, URL http://www.sciencedirect.com/science/article/pii/S0038092X09002667.

T. Otanicar, R. A. Taylor, P. E. Phelan, Prospects for solar cooling – An economic and environmental assessment, Solar Energy 86 (5) (2012) 1287 – 1299, ISSN 0038-092X, URL http://www.sciencedirect.com/science/article/pii/S0038092X12000369.

N. Hartmann, C. Glueck, F. Schmidt, Solar cooling for small office buildings: Comparison of solar thermal and photovoltaic options for two different European climates, Renewable Energy 36 (5) (2011) 1329 – 1338, ISSN 0960-1481, URL http://www.sciencedirect.com/science/article/pii/S0960148110005082.

R. M. Lazzarin, Solar cooling: PV or thermal? A thermodynamic and economical analysis, International Journal of Refrigeration 39 (2014) 38 – 47, ISSN 0140-7007, URL http://www.sciencedirect.com/science/article/pii/S0140700713001394, solar Cooling.

R. Lazzarin, M. Noro, Past, present, future of solar cooling: Technical and economical considerations, Solar Energy 172 (2018) 2 – 13, ISSN 0038-092X, URL http://www.sciencedirect.com/science/article/pii/S0038092X17311374, special issue for Solar Cooling.

U. Eicker, D. Pietruschka, A. Schmitt, M. Haag, Comparison of photovoltaic and solar thermal cooling systems for office buildings in different climates, Solar Energy 118 (2015) 243 – 255, ISSN 0038-092X, URL http://www.sciencedirect.com/science/article/pii/S0038092X15002674.

D. Mugnier, R. Fedrizzi, R. Thygesen, T. Selke, New Generation Solar Cooling and Heating Systems with IEA SHC Task 53: Overview and First Results, Energy Procedia 70 (2015) 470 – 473, ISSN 1876-6102, URL http://www.sciencedirect.com/science/article/pii/S1876610215002714, international Conference on Solar Heating and Cooling for Buildings and Industry, SHC 2014.

A. Al-Alili, Y. Hwang, R. Radermacher, Review of solar thermal air conditioning technologies, International Journal of Refrigeration 39 (2014) 4 – 22, ISSN 0140-7007, URL http://www.sciencedirect.com/science/article/pii/S0140700713003691, solar Cooling.

P. H. Biwole, P. Eclache, F. Kuznik, Phase-change materials to improve solar panel's performance, Energy and Buildings 62 (2013) 59 – 67, ISSN 0378-7788, URL http://www.sciencedirect.com/science/article/pii/S0378778813001539.

M. Chandrasekar, S. Rajkumar, D. Valavan, A review on the thermal regulation techniques for non integrated flat PV modules mounted on building top, Energy and Buildings 86 (2015) 692 – 697, ISSN 0378-7788, URL http://www.sciencedirect.com/science/article/pii/S0378778814009177.

S. Odeh, M. Behnia, Improving Photovoltaic Module Efficiency Using Water Cooling, Heat Transfer Engineering 30 (6) (2009) 499–505, URL https://doi.org/10.1080/01457630802529214.

H. Teo, P. Lee, M. Hawlader, An active cooling system for photovoltaic modules, Applied Energy 90 (1) (2012) 309 – 315, ISSN 0306-2619, URL http://www.sciencedirect.com/science/article/pii/S0306261911000201, energy Solutions for a Sustainable World, Special Issue of International Conference of Applied Energy, ICA2010, April 21-23, 2010, Singapore.

H. Bahaidarah, A. Subhan, P. Gandhidasan, S. Rehman, Performance evaluation of a PV (photovoltaic) module by back surface water cooling for hot climatic conditions, Energy 59 (2013) 445 – 453, ISSN 0360-5442, URL http://www.sciencedirect.com/science/article/pii/S0360544213006567.

A. Kaiser, B. Zamora, R. Mazón, J. García, F. Vera, Experimental study of cooling BIPV modules by forced convection in the air channel, Applied Energy 135 (2014) 88 – 97, ISSN 0306-2619, URL http://www.sciencedirect.com/science/article/pii/S0306261914008903.

S. Chandel, T. Agarwal, Review of cooling techniques using phase change materials for enhancing efficiency of photovoltaic power systems, Renewable and Sustainable Energy Reviews 73 (2017) 1342 – 1351, ISSN 1364-0321, URL http://www.sciencedirect.com/science/article/pii/S1364032117302058.

M. Lucas, F. Aguilar, J. Ruiz, C. Cutillas, A. Kaiser, P. Vicente, Photovoltaic Evaporative Chimney as a new alternative to enhance solar cooling, Renewable Energy 111 (2017) 26 – 37, ISSN 0960-1481, URL http://www.sciencedirect.com/science/article/pii/S0960148117302781.

M. Lucas, J. Ruiz, F. Aguilar, C. Cutillas, A. Kaiser, P. Vicente, Experimental study of a modified evaporative photovoltaic chimney including water sliding, Renewable Energy 134 (2019) 161 – 168, ISSN 0960-1481, URL http://www.sciencedirect.com/science/article/pii/S0960148118313272.

ISO, Solar energy - Specification and classification of instruments for measuring hemispherical solar and direct solar radiation, 2018.

M. Poppe, H. Rögener, Berechnung von Rückkühlwerken, VDI wärmeatlas (1991) Mi 1.

J. Kloppers, D. Kröger, A critical investigation into the heat and mass transfer analysis of counterflow wet-cooling towers, International Journal of Heat and Mass Transfer 48 (3) (2005) 765–777, ISSN 0017-9310.

F. Aguilar, D. Neyer, P. Vicente, Monitoring Procedure for Field Test and Demo Systems with Compression Heat Pumps Driven by Photovoltaic Solar Energy, Tech. Rep., University Miguel Hernández of Elche, URL http://dx.doi.org/10.18777/ieashc-task53-2019-0008, 2018.

P. J. Martínez, J. C. Martínez, M. Lucas, Design and test results of a low-capacity solar cooling system in Alicante (Spain), Solar Energy 86 (10) (2012) 2950 – 2960, ISSN 0038-092X, URL http://www.sciencedirect.com/science/article/pii/S0038092X12002502.

F. Aguilar, D. Crespí-Llorens, P. Quiles, Techno-economic analysis of an air conditioning heat pump powered by photovoltaic panels and the grid, Solar Energy 180 (2019) 169 – 179, ISSN 0038-092X, URL http://www.sciencedirect.com/science/article/pii/S0038092X19300052.

ISO, Guide to the expression of uncertainty in measurement, 1993.

E. Skoplaki, J. Palyvos, On the temperature dependence of photovoltaic module electrical performance: A review of efficiency/power correlations, Solar Energy 83 (5) (2009) 614 – 624, ISSN 0038-092X, URL http://www.sciencedirect.com/science/article/pii/S0038092X08002788.

J. Ruiz, M. P, H. Sadafi, F. Aguilar, J. Toledo, J. Blanes, M. Lucas, Analytical optimization of a solar-driven cooling system enhanced with a photovoltaic evaporative chimney, in: Proceedings of the 14þInternational Conference on Heat Transfer, Fluid Mechanics and Thermodynamics (HEFAT 2019), ISBN 978-1-77592-191-2, 205 – 210, URL https://www.eiseverywhere.com/ehome/349879/943016/login.php?, 2019.

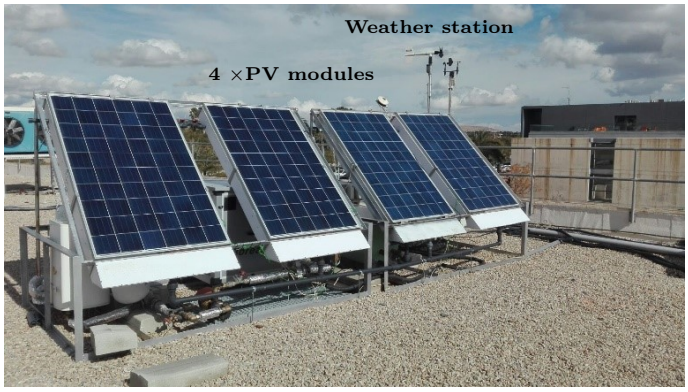

(a)

(b)

Figure 1: Experimental facility located in Torrepinet building, Miguel Hernández University of Elche (Spain). (a) Front side view including the labels of the PV panels and the weather station. (b) Rear side view including the labels of the water-water chiller, evaporative chimneys and electrical heaters.

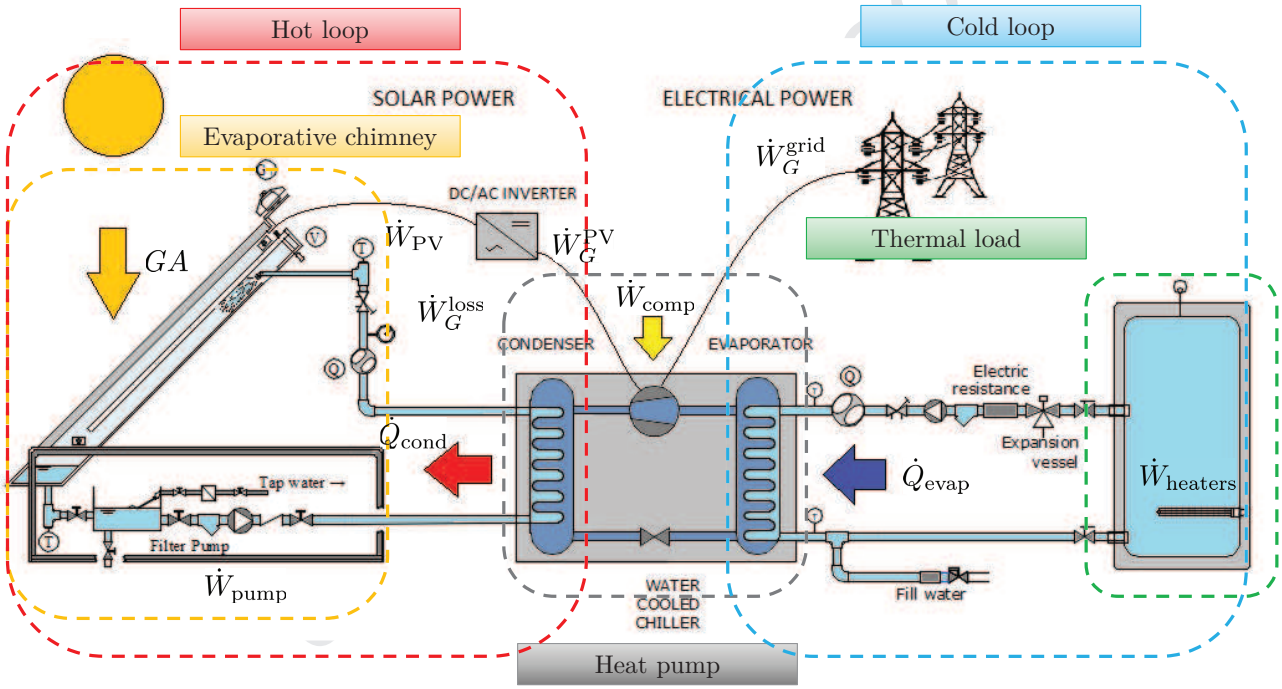

Figure 2: Schematic arrangement of the PV evaporative chimney system and power quantities related to each component.

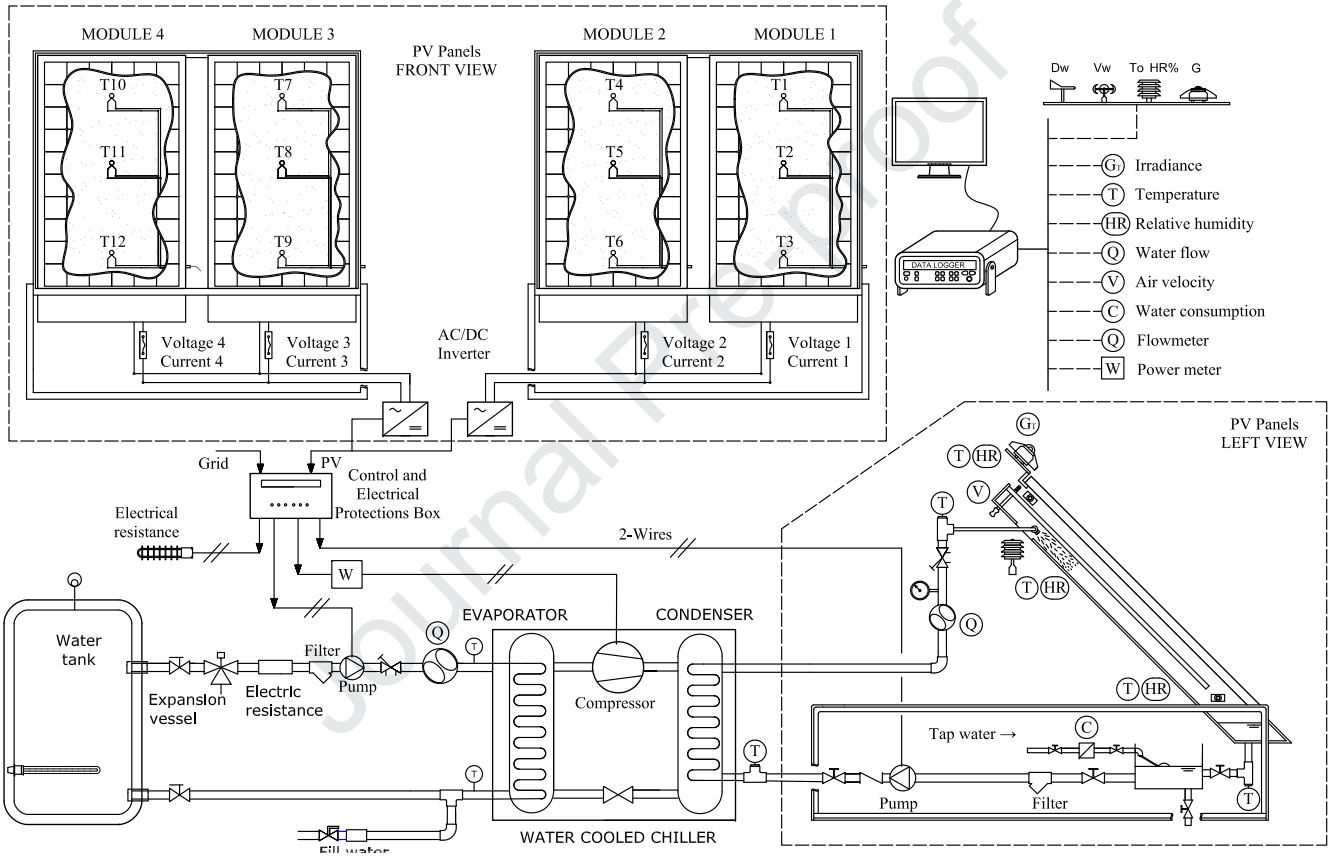

Figure 3: Schematic diagram of the experimental measuring equipment.

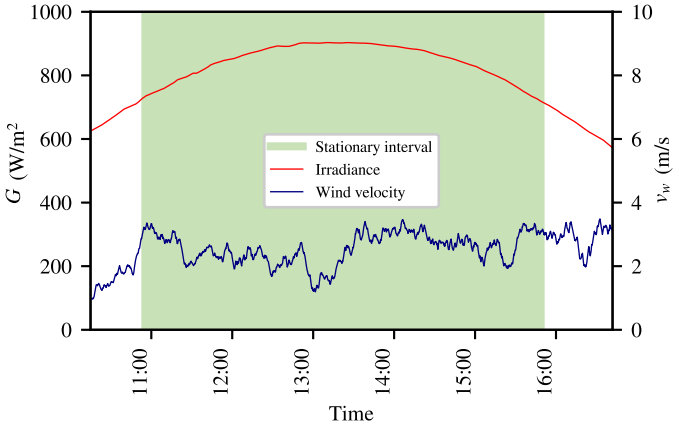

(a) Irradiance and wind velocity for test run 4.

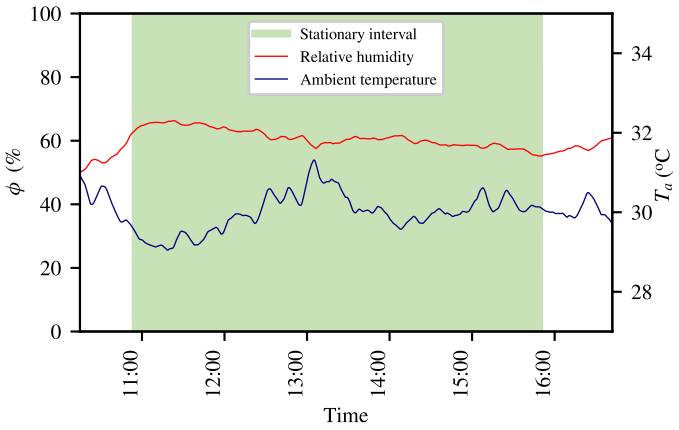

(b) Ambient temperature and relative humidity for test run 4.

Figure 4: Ambient conditions registered during test run 4.

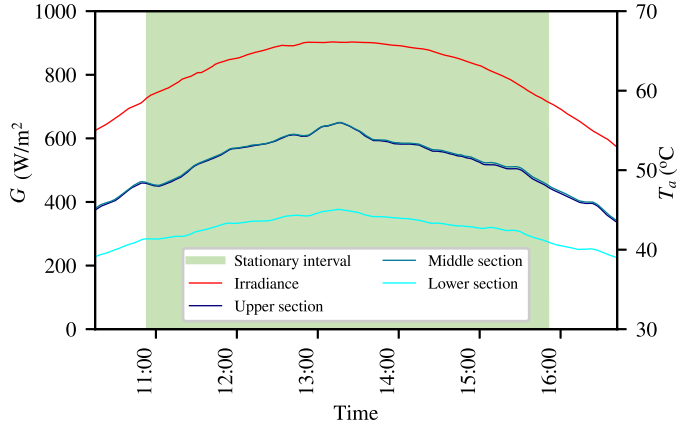

(a) Irradiance and average temperatures distributions for test run 4.

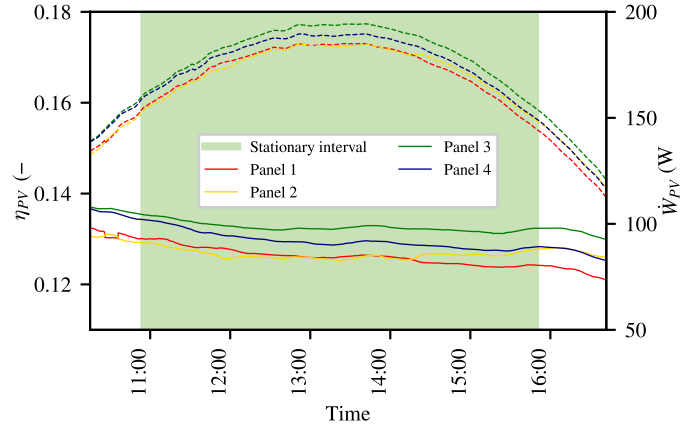

(b) Power generation (dashed lines, right y-axis) and efficiency (solid lines, left y-axis) of the PV panels for test run 4.

Figure 5: Photovoltaic panels' conditions registered during test run 4.

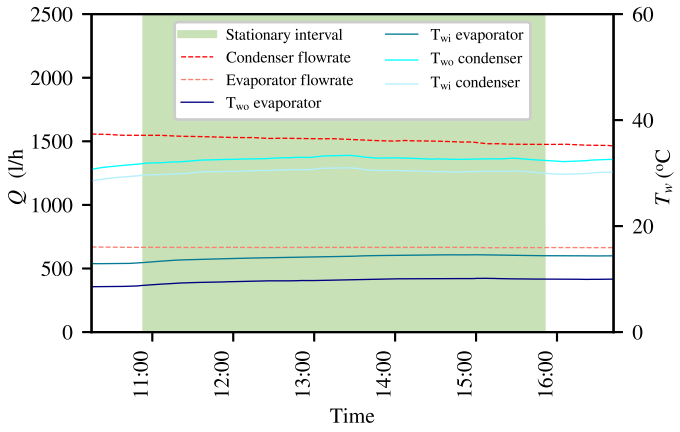

(a) Q (dashed lines, left y-axis) and T_w (solid lines, right y-axis) in evaporator and condenser for test run 4.

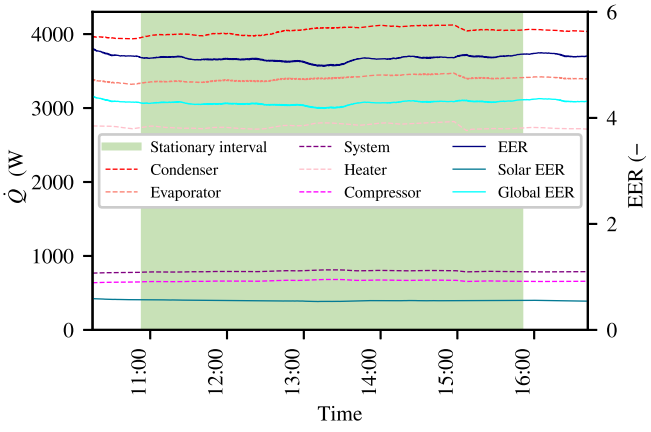

(b) Power balance in the system (dashed lines, left y-axis) and EER's (solid lines, right y-axis) for test run 4.

Figure 6: Heat pump performance parameters during test run number 4.

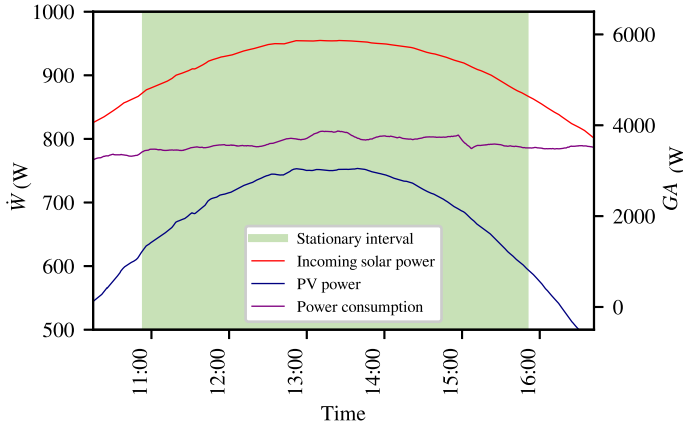

Figure 7: PV generation, total consumption of the system and incoming solar power for test run number 4.

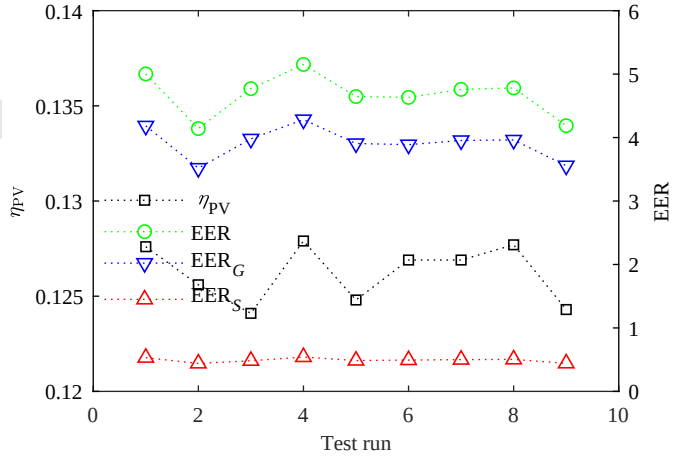

Figure 8: PV panels, heat pump and system performance parameters calculated for all the tests performed.

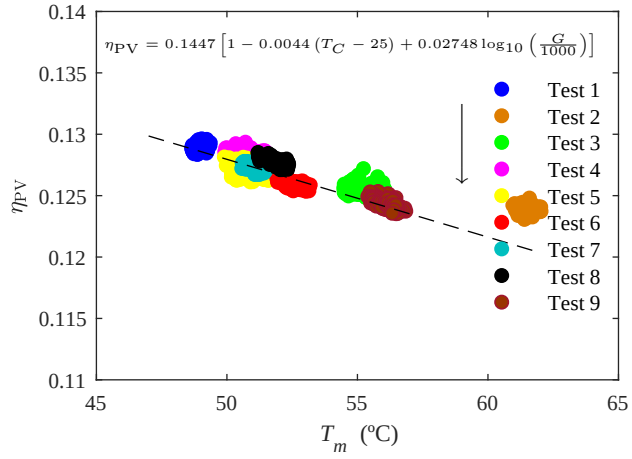

Figure 9: Experimental characterization of the photovoltaic panels performance.

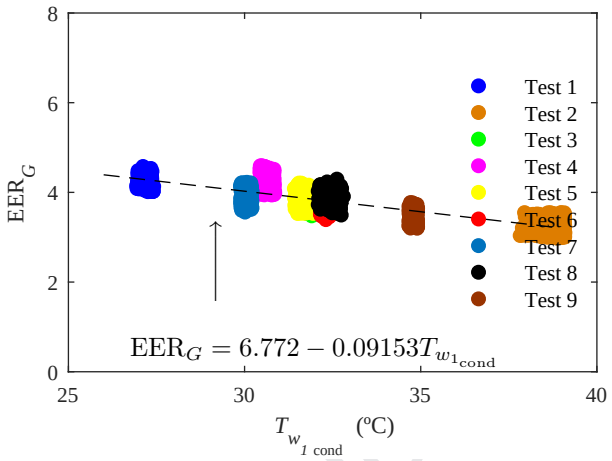

Figure 10: Experimental characterization of the system performance.

This paper evaluates the overall performance of a novel PV solar cooling system

The system's ability to convert solar energy into cooling was, on average, 0.49

The calculated averaged solar contribution was found to be 64.40%

The system produces 11.32 thermal kWh per each kWh consumed from the grid

Declaration of interests

☒ The authors declare that they have no known competing financial interests or personal relationships that could have appeared to influence the work reported in this paper.

☐The authors declare the following financial interests/personal relationships which may be considered as potential competing interests: